International Journal of Heat and Fluid Flow 29 (2008) 1462–1468

Contents lists available at ScienceDirect

International Journal of Heat and Fluid Flow

journal homepage: www.elsevier.com/locate/ijhff

Numerical investigation of the flow of a glass melt through a long circular pipe

Cornelia Giessler, Ruben Schlegel, André Thess *

Department of Mechanical Engineering, Ilmenau University of Technology, P.O. Box 100565, 98684 Ilmenau, Germany

ARTICLE INFO

Article history:
Received 13 March 2007
Received in revised form 23 May 2008
Accepted 9 June 2008
Available online 9 August 2008

Keywords:
Laminar flow
Pipe flow
Numerical simulation

ABSTRACT

This work is concerned with the comparison between a two-dimensional axisymmetric simulation of glass melt flowing through a pipe with a circular cross-section and a one-dimensional model studied by Gießler et al. [Gießler, C., Lange, U., Thess, A., 2007. Nonlinear laminar pipe flow of fluids with strongly temperature-dependent material properties. Phys. Fluids 19, 043602]. The fluid is supposed to be heated by internal electromagnetic (Joule) heating and cooled at the wall by convection. The exponential temperature dependence of the viscosity and the electrical conductivity are fully taken into account. The two models are being compared over a range of values of two different parameters. We find a very good agreement for moderate and high thermal conductivities or in the case of dominating heating. For strong cooling and low thermal conductivities, differences between the one-dimensional model and the two-dimensional axisymmetric simulation occur. The comparison shows that in the latter case the formation of strong radial temperature variations and the resulting radial variation of the viscosity lead to a divergence between the two-dimensional simulation and the one-dimensional model.

1. Introduction

During the production of glass usually Forehearth and Feeder systems are used to transport and condition the glass melt (Noelle, 1997). These are typically pipes or ducts connecting the melting furnace and forming device where the melt is cooled down from the refining temperature to a suitable forming temperature. This is often realized by applying an electrical current either directly into the melt or if the walls are conductive, upon the walls of the pipe. The temperature variation within the melt leads to a large change of various material properties which can lead to unintended inhomogeneities of the final glass product.

In order to control the cooling process we have to obtain a deeper understanding of the behaviour of the system. An accurate prediction of the pipe flow is necessary including all relevant temperature-dependent material parameters. The goal of our work is to show numerically the complex flow structure of a two-dimensional axisymmetric pipe flow if the temperature-dependent material properties of glass melts are included.

There have been several works mainly in geological science focusing on temperature-dependent viscosity. In Richardson (1986), Whitehead and Helfrich (1991), Helfrich (1995), and Wylie and Lister (1995), one-dimensional models of lava flow in slots, ducts or pipes with cooled walls had been derived. These studies observed that the temperature-dependent viscosity can lead to a dramatic modification of the laminar flow characteristics. Bifurcation develops for sufficiently large viscosity differences – for a given pressure drop three steady state solutions were found. Similar results were found for a pipe flow of glass melts in Lange and Loch (2002) and reported from glass production (Lange, private communication). In all these works only non-heated flows in cooled tubes were considered. Heating, however, has not been considered at all. A recent theoretical contribution (Gießler et al., 2007) examined the influence of coupled wall heat loss and internal volumetric heating. Furthermore, this work included the full non-linear temperature dependence of the viscosity and electrical conductivity. In this one-dimensional model of glass melt the flow is driven by a constant external force density which is acting along the whole pipe. Additionally, the flow is influenced by temperature variations due to wall heat loss, internal heating, advection, and diffusion. The model allows the calculation of the mean velocity and the mean temperature for a given set of parameters. While a bifurcation develops when the fluid is cooled, a non-linear laminar flow characteristic develops when the fluid is heated. However, this analytical model neglects the dependence of velocity and temperature on the radial coordinate which may influence the flow as well.

The goal of the present work is to validate this one-dimensional model and to analyse the influence of the dependence of velocity and temperature on the radial coordinate. In order to achieve this goal we systematically perform numerical parameter studies of the pipe flow model using a two-dimensional axial configuration. We would like to find the range of validity for the one-dimensional model. Furthermore, we will explain physically deviations of the numerically and analytically obtained results.

* Corresponding author. Tel.: +49 3677 69 2445; fax: +49 3677 69 1281.
E-mail address: thess@tu-ilmenau.de (A. Thess).

0142-727X/$ - see front matter © 2008 Elsevier Inc. All rights reserved.
doi:10.1016/j.ijheatfluidflow.2008.06.001

Nomenclature

A	glass-specific viscosity parameter	T_{in}	inlet temperature (K)
B	glass-specific viscosity parameter (K)	T_{out}	mean outlet temperature (K)
C	glass-specific viscosity parameter (°C)	$\boldsymbol{u}(x,r)$	velocity field (m/s)
c_p	heat capacity (J/(kg K))	u_m	mean velocity (m/s)
E	glass-specific constant	x,r	system of coordinates (m)
F	glass-specific constant (K)	λ	thermal conductivity (W/m K)
G	glass-specific constant (°C)	η	dynamic viscosity (Pa s)
$\boldsymbol{J}$	current density (A/m^2)	η_0	glass-specific viscosity parameter (Pa s)
L	length of the pipe (m)	α	heat-transfer coefficient (W/m^2 K)
p_{diff}	mean pressure difference (Pa)	ρ	density (kg/m^3)
R	radius of the pipe (m)	σ	electrical conductivity (S/m)
T	temperature (K)	σ_0	glass-specific constant (S/m)
T_∞	ambient temperature (K)		

2. Mathematical formulation and numerical method

2.1. Definition of the model

We consider a laminar and steady flow of a viscous electrically conducting fluid in a pipe with circular cross-section driven by a pressure difference between the inlet and the outlet of the pipe. The pipe has the length L and the radius $R \ll L$ as shown in Fig. 2-1. At the inlet of the pipe the temperature T_{in} and the parabolic flow profile with the mean velocity $u_m = u_{max}/2$ are given. An external homogenous horizontal electric current density $\boldsymbol{J}$ acts upon the entire circular pipe. The Joule heat flux density $J^2/\sigma(T)$ acts as an energy source.

The highly viscous fluid with constant density ρ is supposed to have strongly temperature-dependent viscosity $\eta(T)$ and electrical conductivity $\sigma(T)$. During the simulations the temperature-dependent viscosity equation,

$$\eta(T) = \eta_0 \cdot \exp(-A + B/(T + C)), \tag{1}$$

and the equation for the temperature-dependent electrical conductivity

$$\sigma(T) = \sigma_0 \cdot \exp(E - F/(T + G)) \tag{2}$$

are used. The constant parameters A, B, C, E, F, G are specific to the considered glass melt. While the viscosity decreases as the temperature increases, the electrical conductivity increases significantly with the temperature. As C is typically negative, the viscosity law Eq. (1) only makes sense for $T > -C$ as $\eta \to \infty$ for $T \to |C|$.

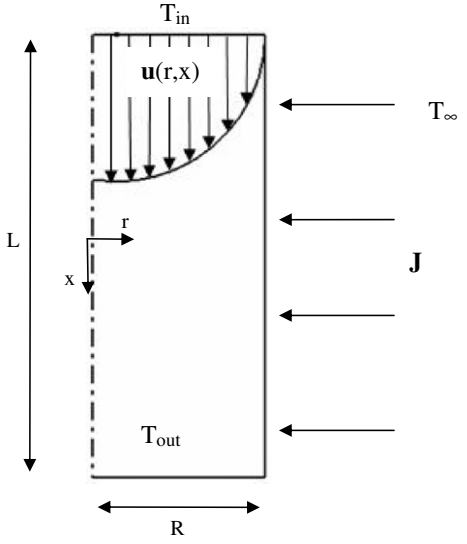

Fig. 2-1. Sketch of the considered flow in a circular pipe.

The steady pipe flow is governed by the steady Navier–Stokes equation,

$$\rho u \cdot (\nabla u) = -\nabla p + \nabla \cdot [\eta(\nabla u + (\nabla u)^T)], \tag{3}$$

and the condition of incompressibility

$$\nabla \cdot u = 0. \tag{4}$$

The left hand-side of the Stokes Eq. (3) represents the advection of the velocity field and the right hand-side represents the driving pressure gradient and the internal friction. We like to emphasize, that the velocity field $\boldsymbol{u} = u_r(x,r)\boldsymbol{e}_r + u_x(x,r)\boldsymbol{e}_x$ is not only a function of the radial coordinate r. As the viscosity is a function of the temperature and therefore depends both on r and x, the velocity $\boldsymbol{u}$ depends on the axial position as well, e.g. $\boldsymbol{u} = \boldsymbol{u}(x,r)$. As a result the flow is not fully developed. The applied boundary conditions of the two-dimensional axial model are

$$\frac{\partial u_x}{\partial r} = 0, \quad u_r = 0, \quad \text{for } r = 0, \tag{5a}$$

$$u_r = u_x = 0 \quad \text{for } r = R, \tag{5b}$$

$$u_x = 2 \cdot u_m \cdot \left(1 - \left(\frac{r}{R}\right)^2\right), \quad u_r = 0 \quad \text{for } x = 0, \tag{5c}$$

$$u_r = 0, \quad p = 0 \quad \text{for } x = L. \tag{5d}$$

Let us note that the boundary condition at the outlet, Eq. (5d), is the outflow condition which is provided by the commercial tool Comsol.

To calculate the temperature distribution in the pipe the steady energy equation

$$\rho c_p u \cdot \nabla T = \frac{J^2}{\sigma(T)} + \lambda \cdot \nabla^2 T \tag{6}$$

applies with the boundary conditions given by

$$\frac{\partial T}{\partial r}(0,x) = 0 \quad \text{for } r = 0, \tag{7a}$$

$$-\lambda \frac{\partial T(R,x)}{\partial r} = \alpha(T(R,x) - T_\infty) \quad \text{for } r = R, \tag{7b}$$

$$T(r,0) = T_{in} \quad \text{for } x = 0, \tag{7c}$$

$$\boldsymbol{e}_x \cdot (-k\nabla T) = 0 \quad \text{for } x = L. \tag{7d}$$

The heat convection is specified on the left-hand side of the energy Eq. (6) with the constant density ρ and the constant heat capacity c_p. The first term on the right-hand side represents the generation of heat by the Joule effect according to $J^2/\sigma(T)$. The second term specifies the heat conduction with constant thermal conductivity

coefficient λ. The boundary condition, Eq. (7b), specifies the convective heat-transfer at the pipe wall with the external temperature T_∞ and the constant overall heat-transfer coefficient α. A short explanation of the validity of this boundary condition is given in the Appendix.

2.2. Numerical method

The purpose of this work is to verify the results of the analytic one-dimensional model studied in Gießler et al. (2007). This model describes the variables only as function of the coordinate x. For example the calculation of the mean viscosity in Gießler et al. (2007) is done exclusively with the mean temperature. The present numerical analysis using the commercial software package COMSOL, however, predicts the dependence of $\boldsymbol{u}$ and T on two coordinates, namely the streamwise coordinate x and the radial coordinate r. As a result, a temperature- and viscosity-profile are established at every x by the additional consideration of the dependence on r.

In the process of our numerical study the mean velocity u_m and the inlet temperature T_{in} are prescribed. The output quantities we analysed are the mean pressure difference p_{diff} that arises between in- and outlet of the cylinder and the mean temperature at the outlet T_{out}. To determine the pressure at the in- and outlet an integration is carried out. The mean pressure difference is a cross-section averaged quantity and is defined as follows:

$$p_{diff} = \frac{2}{R^2}\left(\int_0^R p(r,0)r\mathrm{d}r - \int_0^R p(r,L)r\mathrm{d}r\right).$$

A similar definition applies for the cross-section averaged temperature at the outlet:

$$T_{out} = \frac{2}{R^2}\int_0^R T(r,L)r\mathrm{d}r.$$

The multiphysics tool COMSOL uses the finite-element method to solve partial differential equations. We use the direct solver UMFPACK with a relative accuracy of 1.0E−6. The mesh is unstructured with a total of 4480 basic net elements, whereas the border areas of the cylinder have a more detailed resolution because of the complexity of the computations. Tests of convergence for the two-dimensional axial model at hand led to the following result: a number of only 2000 basic net elements already produce converged results as shown in Fig. 2-2.

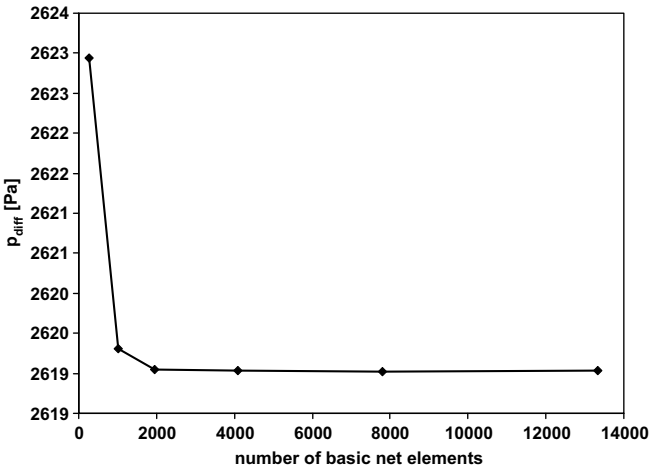

Fig. 2-2. Convergence behaviour of the pressure difference as a function of the number of basic net elements for two-dimensional axisymmetric simulation with $J = 10^3$ A/m^2, $T_\infty = 293.15$ K, $u_m = 10^{-5}$ m/s.

We checked our numerical model by calculating the mean velocity for a given pressure difference for an isothermal case. The results match with results obtained with the Hagen–Poiseulle law (White, 1999).

3. Results

In our studies the current density $\boldsymbol{J}$, the heat-transfer coefficient α and the ambient temperature T_∞ are varied to verify the validity of the one-dimensional model in a wide range of parameters. For an easy comparability with the one-dimensional model (Gießler et al., 2007) only the temperature dependence of the viscosity $\eta(T)$ and of the electrical conductivity $\sigma(T)$ are taken into account. All other material parameters are treated as constants. Typically glass has a temperature-dependent thermal conductivity $\lambda(T)$. But the main object of the one-dimensional model was to study the influence of the temperature-dependent electrical conductivity and viscosity on the flow. Therefore, and to keep the one-dimensional model as simple as possible, λ is set to a constant value. In the following simulation the thermal conductivity is assumed to be constant to allow for a good comparability. During the studies in Section 3.4 simulations for different λ values are carried out to analyse its effect on the fluid flow. The calculations are carried out for the SCHOTT glass nb. 8412 – "Fiolax klar" with the material properties given in Table 1. The examined pipe has a radius of $R = 0.025$ m, a length of $L = 0.5$ m and an inlet temperature of $T_{in} = 1573.15$ K.

3.1. Heating without cooling

First we examine a system with heating due to the Joule effect and without cooling, $\alpha = 0$ W/m^2 K. The dependence of the mean inlet velocity u_m and mean outlet temperature T_{out} on the applied mean pressure difference p_{diff} is shown in Figs. 3-1 and 3-2, respectively. We performed two analysis for $J_1 = 10^3$ A/m^2 and $J_2 = 10^4$ A/m^2, respectively. Starting with a high velocity u_m the pressure difference p_{diff} is found to decrease linearly. A similar linear flow characteristic is observed if we start with a low velocity. The transition between these linear regimes is characterised by a non-linear regime. For high velocities the flow characteristic does not depend on the heat input, so the curves for J_1 and J_2 coincide. But for small velocities the curves are shifted for different heat inputs. Here the pressure difference for a given velocity is smaller if the heat input is higher. The lower linear flow regime is a consequence of the weak variation of the viscosity, as η approaches asymptotically its lowest possible value $\eta(T) = \eta_0$ for high temperatures. Only a higher current density leads to a further rise of the temperature until the influence compared with the heat conduction is so low, that a constant maximum temperature arises, see Fig. 3-2.

The comparison of the simulation results (markers in Figs. 3-1 and 3-2) with the results obtained with the one-dimensional model (lines in Figs. 3-1 and 3-2) shows a very good agreement. This is

Table 1
Material parameters for the SCHOTT glass nb. 8412 "Fiolax klar"

c_p	1450
ρ	2200
A	2.30259
B	10679.4
C	−242.2
E	2.04117
F	7680.11
G	273.15
σ_0	100
η_0	0.1
λ	1.2

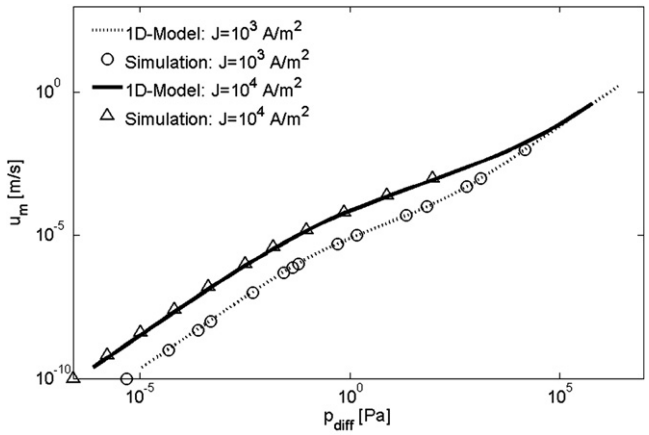

Fig. 3-1. Results for heating without cooling: dependence of the mean velocity on the applied pressure difference as obtained from the numerical simulation for $J = 10^3$ A/m^2 and for $J = 10^4$ A/m^2 in comparison with the prediction of the one-dimensional model of Gießler et al. (2007) with $\alpha = 0$ W/m^2 K.

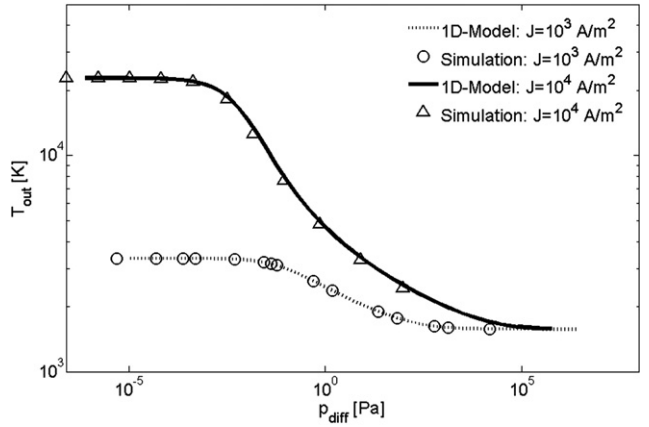

Fig. 3-2. Results for heating without cooling: dependence of the mean outlet temperature on the applied pressure difference as obtained from the numerical simulation for $J = 10^3$ A/m^2 and for $J = 10^4$ A/m^2 in comparison with the prediction of the one-dimensional model of Gießler et al. (2007) with $\alpha = 0$ W/m^2 K, and $T_{in} = 1573.15$ K.

due to the fact that the Joule heating warms up the fluid homogenously and according to that the dependence of the temperature on r is weak. Therefore, the radial variation of η is small and the mean viscosity of the two-dimensional simulation and the one-dimensional model coincide.

3.2. Cooling without heating

In this Section we turn to a system with cooling, $\alpha = 10$ W/m^2 K, and without heating, e.g. $J = 0$ A/m^2. In doing so, we vary u_m as well as the ambient temperature T_∞ and calculate the mean pressure difference p_{diff} between the inlet and the outlet and the mean outlet temperature T_{out}. The results are shown in Figs. 3-3 and 3-4.

For a high ambient temperature of $T_\infty = 1173.73$ K we observe a bifurcation, hence a pressure range in which one pressure value can be assigned to three different velocities. For a low ambient temperature of $T_\infty = 293.73$ K a double valued solution exists. It means that for moderate and large pressure differences two velocities are obtained for one set of parameters. There is a minimal pressure difference p_{diff} at which one pressure difference p_{diff} matches unambiguously with one velocity u_m. For very small pressure differences the strong cooling leads to $T \to |C|$. As a result we have $\eta \to \infty$, see Eq. (1), and no solution of the governing Eqs. (3)–(7) exists at all. Hence, the lower branch of the curve is missing.

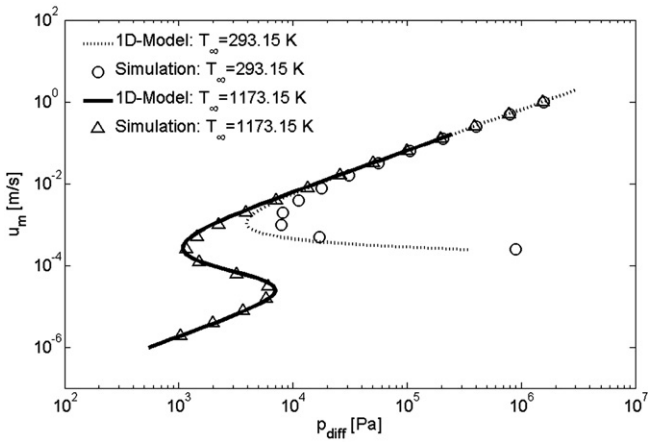

Fig. 3-3. Results for cooling without heating: dependence of the mean velocity on the applied pressure difference as obtained from the numerical simulation for $T_\infty = 293.15$ K and for $T_\infty = 1173.15$ K in comparison with the prediction of the one-dimensional model of Gießler et al. (2007) with $\alpha = 10$ W/m^2 K.

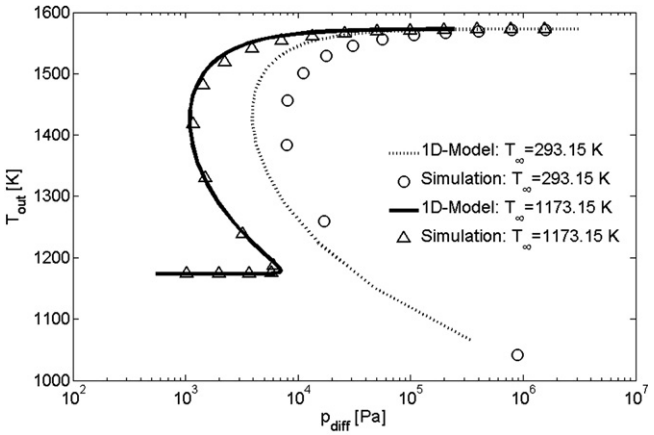

Fig. 3-4. Results for cooling without heating: dependence of the mean outlet temperature on the applied pressure difference as obtained from the numerical simulation for $T_\infty = 293.15$ K and for $T_\infty = 1173.15$ K in comparison with the prediction of the one-dimensional model of Gießler et al. (2007) with $\alpha = 10$ W/m^2 K, and $T_{in} = 1573.15$ K.

Figs. 3-3 and 3-4 further show that the results obtained with the two models are in a good agreement. For the high ambient temperature the quantitative agreement is particularly noteworthy.

The difference between the results of the simulations and the one-dimensional model for the cooling temperature $T_\infty = 293.73$ K originates from the radial variation of the temperature and finally the radial variation of the viscosity. In the one-dimensional model the viscosity is calculated for the mean temperature, whereas in the simulation the full radial temperature distribution and the non-linear temperature-dependent viscosity in radial direction are considered. Fig. 3-5 shows that for a given velocity of $u_m = 10^{-3}$ m/s the outlet temperature predicted by the one-dimensional model is equal to the mean outlet temperature obtained with the two-dimensional simulation. However, in the simulation the strong cooling at the pipe wall has a significant influence. As the viscosity increases exponentially with decreasing temperature, the viscosity in the vicinity of the wall increases much more than with a linear temperature dependence. Consequently, the mean viscosity in the simulation is higher than the mean viscosity in the one-dimensional model as indicated apparent in Fig. 3-6. For this reason a higher driving pressure difference p_{diff} is necessary in the simulation during the reduction of the

temperature to obtain the same velocities as in the analytical one-dimensional model. Therefore the inflexion point is reached at a higher p_{diff} in the two-dimensional simulation.

Because of the variation in radial and axial direction of the viscosity in the pipe, the velocity profile changes as well, see Fig. 3-7. It is readily seen that the prescribed parabolic velocity profile exists only at the inlet. With increasing cooling along the pipe axis – and hence an increasing viscosity at the pipe walls – the velocity at the edge decreases. In return, due to the condition of incompressibility, the velocity increases toward the centre of the pipe. Therefore the velocity profile at the outlet is squeezed.

3.3. Heating and cooling at different heat-transfer coefficients

In Section 3.3 we deal with the general case which consists of cooling of the fluid while it is heated at the same time. In the process we vary the heat-transfer coefficient α and keep all other parameters constant, i.e. the ambient temperature is set to $T_\infty = 293.73$ K and the current density is set to $J = 10^3$ A/m^2. The results of the simulations are summarized in Figs. 3-8 and 3-9.

For a heat-transfer coefficient of $\alpha = 1$ W/m^2 K the influence of the heating is still stronger than that of the cooling. The dependence of u_m on p_{diff} looks similar like the case of pure heating we discussed in Section 3.1. If cooling dominates, $\alpha = 10$ W/m^2 K and $\alpha = 50$ W/m^2 K, a bifurcation develops. Because of the additional heating we do not receive a two valued solution like in Section 3.2. With increasing cooling of the fluid the bifurcation is more pronounced and the quantitative differences between the simulation and the one-dimensional model increases. The range in which one pressure value can be assigned to three velocities is much smaller in the simulation than in the one-dimensional model, as it can be seen in Fig. 3-8. In the upper branch, coming from a high velocity, bifurcation sets in for larger p_{diff} in the simulation. An explanation for this behaviour can be found in the strong cooling of the melt at the wall and the accompanying increase of the viscosity, like in the case of cooling without heating we discussed in Section 3.2.

3.4. Cooling and heating at different thermal conductivities

Finally we study the general case involving cooling and heating at different thermal conductivities λ. Again, the ambient temperature is set to $T_\infty = 293.15$ K and the heat-transfer coefficient is set

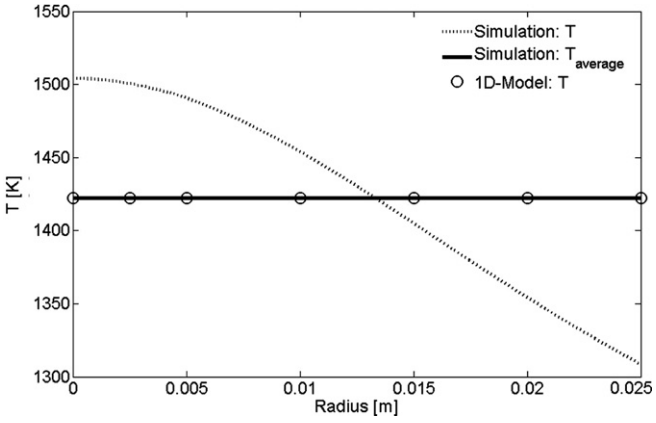

Fig. 3-5. Radial profile of the temperature for the case of cooling without heating: temperature $T(L,r)$ (dotted line) and mean temperature T_{out} as obtained from the present simulation in comparison with the temperature (circles) predicted by the one-dimensional model with $u_m = 0.001$ m/s, $T_\infty = 293.15$ K, $\alpha = 10$ W/m^2 K, and $T_{in} = 1573.15$ K.

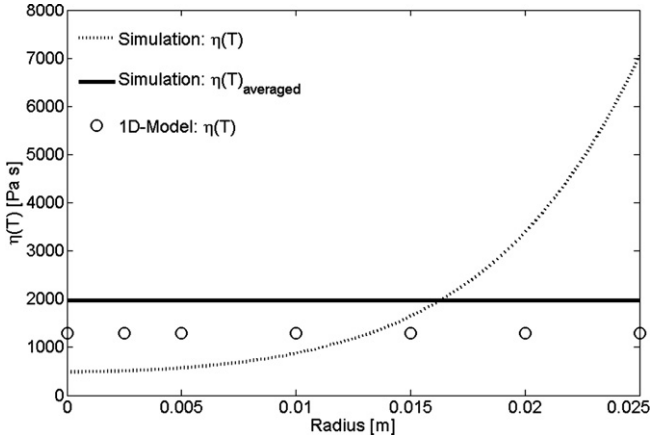

Fig. 3-6. Radial profile of the viscosity for the case of cooling without heating: viscosity $\eta(L,r)$ (dotted line) and mean viscosity at the outlet η_{out} as obtained from the present simulation in comparison with the viscosity (circles) predicted by the one-dimensional model with $u_m = 0.001$ m/s, $T_\infty = 293.15$ K $\alpha = 10$ W/m^2 K, and $T_{in} = 1573.15$ K.

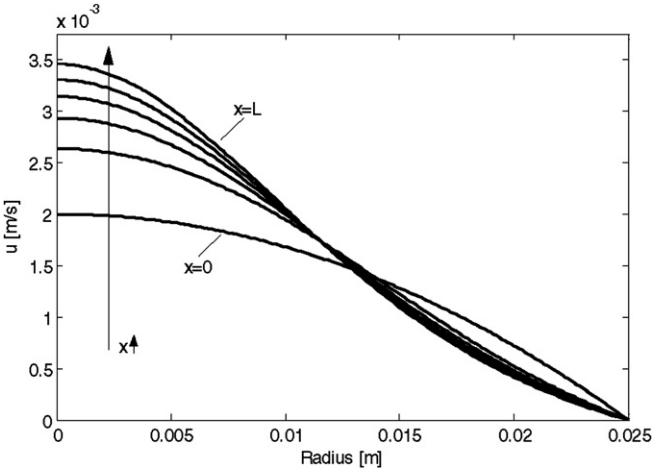

Fig. 3-7. Radial profile of the axial velocity u_x at equidistant positions along the pipe axis including the inlet and the outlet for the case of cooling without heating obtained by numerical simulations with $u_m = 10^{-3}$ m/s, $T_\infty = 293.15$ K, $\alpha = 10$ W/m^2 K, $T_{in} = 1573.15$ K and $x = 0$, $L/5$, $2L/5$, $3L/5$, $4L/5$, L.

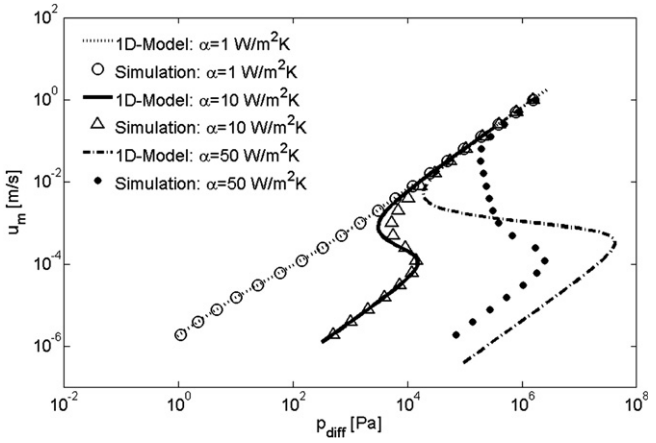

Fig. 3-8. Results for heating and cooling at different heat-transfer coefficients: dependence of the mean velocity on the applied pressure difference as obtained from the numerical simulation for $\alpha = 1$ W/m^2 K, $\alpha = 10$ W/m^2 K and $\alpha = 50$ W/m^2 K in comparison with the prediction of the one-dimensional model of Gießler et al. (2007) with $T_\infty = 293.73$ K, $J = 10^3$ A/m^2.

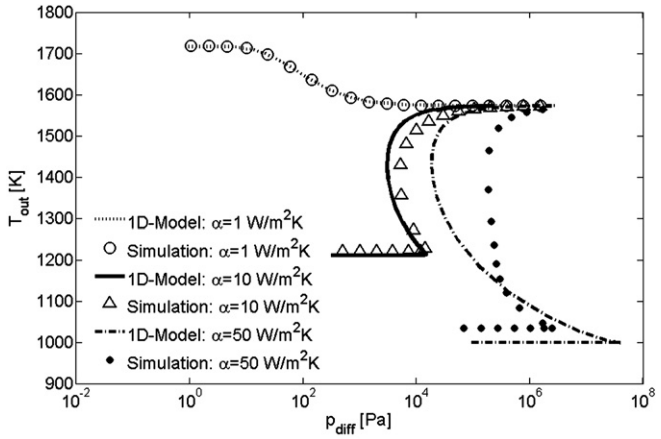

Fig. 3-9. Results for heating and cooling at different heat-transfer coefficients: dependence of the mean outlet temperature on the applied pressure difference as obtained from the numerical simulation for $\alpha = 1\ \mathrm{W/m^2\,K}$, $\alpha = 10\ \mathrm{W/m^2\,K}$ and $\alpha = 50\ \mathrm{W/m^2\,K}$ in comparison with the prediction of the one-dimensional model of Gießler et al. (2007) with $T_\infty = 293.73$ K, $J = 10^3\ \mathrm{A/m^2}$, and $T_{in} = 1573.15$ K.

to $\alpha = 10\ \mathrm{W/m^2\,K}$. The heating of the fluid is accomplished by a current density of $J = 10^3\ \mathrm{A/m^2}$.

If we vary the thermal conductivity λ of the fluid, the flow characteristics can change considerably as one can see in Figs. 3-10 and 3-11. In the one-dimensional model bifurcation develops if the conductivity is smaller than a certain critical value, i.e. $\lambda < \lambda_{max}$. The smaller λ, the more distinct the bifurcation is. For $\lambda = 0$ the pressure range for which one pressure value can be assigned to three velocities reaches its maximum. In contrast in the simulation we obtain a range $\lambda_{min} \leqslant \lambda \leqslant \lambda_{max}$ for which the function $u_m(p_{diff})$ is not single valued. For $\lambda < \lambda_{min}$ and $\lambda > \lambda_{max}$ every p_{diff} can be assigned unambiguously to one u_m.

The results of both models are in good agreement for moderate and large values of λ. This is caused by the flattening of the temperature profile in the simulation with increasing thermal conductivity. If λ has reached a certain value, the temperature in radial direction is almost constant. The agreement of the simulation and the one-dimensional model is very good. Fig. 3-12 shows an example of the flattening of the temperature profile for increasing thermal conductivity.

4. Summary and prospects

This work is concerned with the comparison of a one-dimensional model (Gießler et al., 2007) and a two-dimensional axisymmetric simulation of glass melt flowing through a circular pipe. We assume that the fluid is heated by internal volumetric (Joule) heating and cooled at the wall. The exponential temperature dependence of the viscosity and the electrical conductivity are fully taken into account. While varying different parameters the results

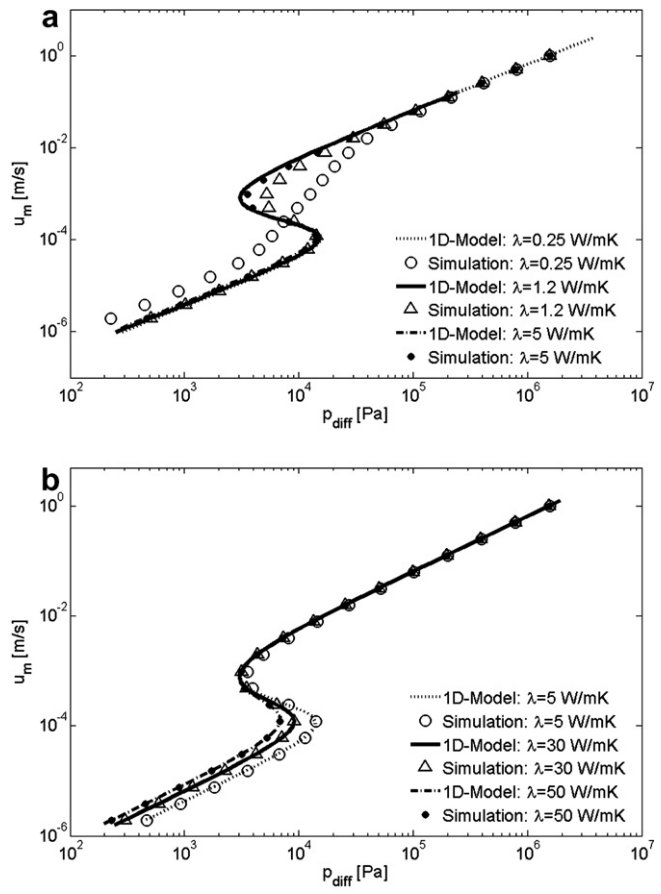

Fig. 3-10. Results for heating and cooling at different thermal conductivities: dependence of the mean velocity on the applied pressure difference as obtained from the numerical simulation for (a) $\lambda = 0.25\ \mathrm{W/m^2\,K}$, $\lambda = 1.2\ \mathrm{W/m^2\,K}$, $\lambda = 5\ \mathrm{W/m^2\,K}$ and (b) $\lambda = 5\ \mathrm{W/m^2\,K}$, $\lambda = 30\ \mathrm{W/m^2K}$, $\lambda = 50\ \mathrm{W/m^2\,K}$ in comparison with the prediction of the one-dimensional model of Gießler et al. (2007) with $T_\infty = 293.73$ K, $\alpha = 10\ \mathrm{W/m^2\,K}$ and $J = 10^3\ \mathrm{A/m^2}$.

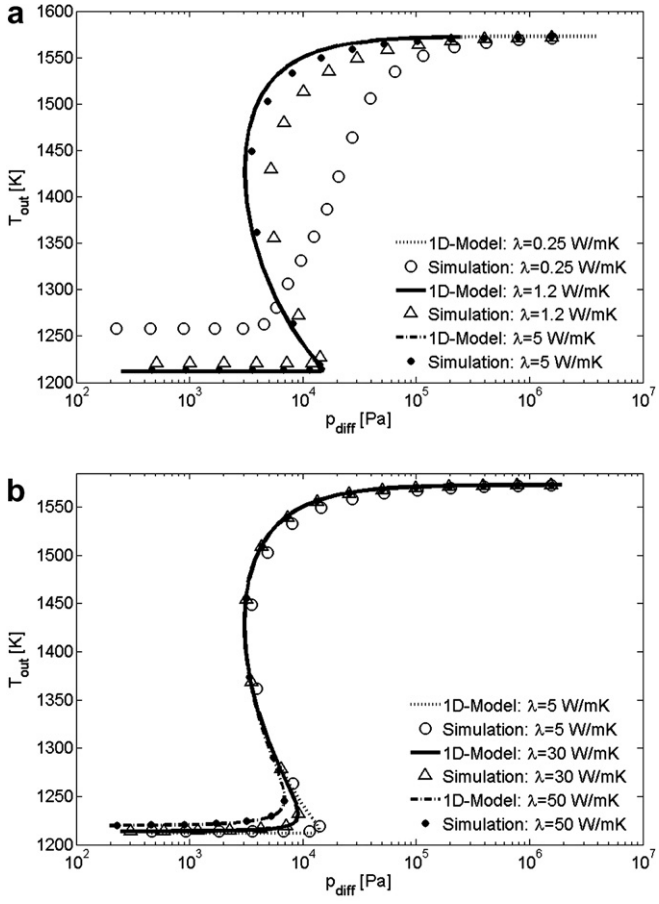

Fig. 3-11. Results for heating and cooling at different thermal conductivities: dependence of the mean outlet temperature on the applied pressure difference as obtained from the numerical simulation for (a) $\lambda = 0.25\ \mathrm{W/m^2\,K}$, $\lambda = 1.2\ \mathrm{W/m^2\,K}$, $\lambda = 5\ \mathrm{W/m^2\,K}$ and (b) $\lambda = 5\ \mathrm{W/m^2\,K}$, $\lambda = 30\ \mathrm{W/m^2\,K}$, $\lambda = 50\ \mathrm{W/m^2\,K}$ in comparison with the prediction of the one-dimensional model of Gießler et al. (2007) with $T_\infty = 293.73$ K, $\alpha = 10\ \mathrm{W/m^2\,K}$, $J = 10^3\ \mathrm{A/m^2}$, and $T_{in} = 1573.15$ K.

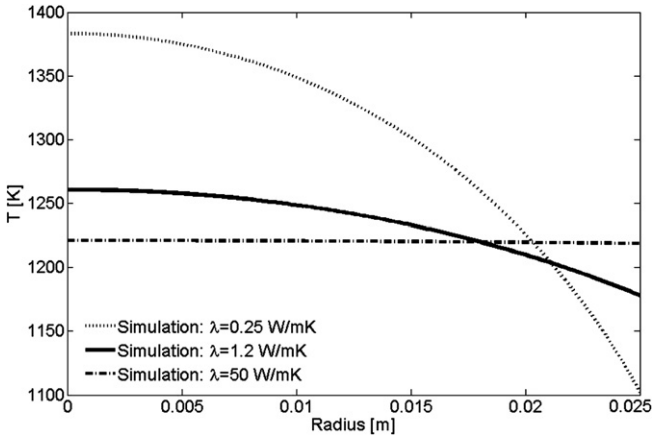

Fig. 3-12. Temperature profile at the outlet $T(L,r)$ for different thermal conductivities λ with $u_m = 10^{-6}$ m/s, $T_\infty = 293.15$ K, $\alpha = 10$ W/m^2 K, $J = 10^3$ A/m^2, and $T_{in} = 1573.15$ K.

of the two models are being compared. The anticipated flow characteristics obtained with the one-dimensional model have been confirmed qualitatively by the two-dimensional axial simulation.

We find a very good agreement between the one-dimensional model and the two-dimensional axisymmetric simulation in the case of heating of the glass melt without cooling. The monotonic, non-linear flow behaviour has been reproduced correctly by the one-dimensional model. In the case of dominating cooling bifurcations develop, which are reproduced by both models. For strong cooling differences between the one-dimensional model and the two-dimensional axial simulation appear. This is a result of large temperature gradients along the radial axis of the pipe and the exponential increase of viscosity with decreasing temperature. The mean viscosity of the simulation is larger than the viscosity obtained with the one-dimensional model. For moderate and high thermal conductivities λ the results of simulation and one-dimensional model are in good agreement, as the temperature is almost constant across the cross-section in the simulation. However, for low thermal conductivity differences develop. In the one-dimensional model bifurcation exists for all $\lambda \leqslant \lambda_{max}$. But in the simulation we observed monotonic flow characteristics for very small λ. Here, bifurcation exists only for $\lambda_{min} \leqslant \lambda \leqslant \lambda_{max}$.

The comparison of both variants for studying the flow characteristics of a circular pipe with coupled physical problems shows positive aspects for the one-dimensional model with respect to computational efficiency and good reproduction of elementary physical phenomena. However, the one-dimensional model does not reproduce the radial dependence of the temperature and the resulting radial viscosity variation. Those are better captured by the two-dimensional finite-element simulation.

Acknowledgements

The authors wish to acknowledge the financial support of the Deutsche Forschungsgemeinschaft under Grant No. TH 497/19-2. We thank U. Lange, D. Hülsenberg, B. Halbedel and U. Krieger for useful discussions and H. Schwanbeck for technical help.

Appendix

In the following the validity of the boundary condition Eq. (7b) at the pipe wall will be explained. Therefore we analyse the effective thermal resistance R_{eff} of the pipe. It is the sum of the resistance for heat conduction through the pipe wall

$$R_{cond} = \ln\left(\frac{R_{out}}{R}\right)\frac{1}{2\pi L\lambda_{wall}}$$

and the resistance for heat convection at the outer side of the wall

$$R_{conv} = \frac{1}{2\pi L R_{out}\alpha},$$

with R_{out} being the outer radius of the pipe, λ_{wall} being the thermal conductivity of the wall and the constant heat-transfer coefficient α, see for example (Incropera and DeWitt, 1996). Now we model the effective resistance $R_{eff} = R_{cond} + R_{conv}$ as effective heat convection

$$R_{eff} = \frac{1}{2\pi L R_{out}\alpha_{eff}}.$$

The effective heat-transfer coefficient α_{eff} then becomes

$$\alpha_{all} = \frac{\alpha}{1 + \ln(R_{out}/R)R_{out}\alpha/\lambda_{wall}}.$$

Typically the thermal conductivity of such pipes in glass production is $\lambda_{wall} \approx 10^2$ W/(m K) and the thickness is about $R_{out} - R \approx 10^{-2}$ m. With a typical radius of $R = 0.025$ m and a typical heat-transfer coefficient of $\alpha \approx 5$ for free convection we have $\ln(R_{out}/R)R_{out}\alpha/\lambda_{wall} \to 1$ which leads to $\alpha_{eff} \approx \alpha$. Therefore it is legitimate to use Eq. (7b) at the wall boundary of the solution area.

References

Gießler, C., Lange, U., Thess, A., 2007. Nonlinear laminar pipe flow of fluids with strongly temperature-dependent material properties. Phys. Fluids 19, 043601.
Helfrich, K.R., 1995. Thermo-viscous fingering of flow in a thin gap: a model of magma flows in dikes and fissures. J. Fluid Mech. 305, 219–238.
Incropera, F.P., DeWitt, D.P., 1996. Fundamentals of Heat and Mass Transfer. Wiley, New York.
U. Lange, private communication.
Lange, U., Loch, H., 2002. Instabilities and stabilization of glass pipe flow. In: Krause, D., Loch, H. (Eds.), Mathematical Simulation in Glass Technology, Schott Series on Glass and Glass Ceramics. Springer-Verlag, Berlin.
Noelle, G., 1997. Technik der Glasherstellung. Deutscher Verlage für Grundstoffindustrie, Stuttgart.
Richardson, S.M., 1986. Injection moulding of thermoplastics: freezing of variable-viscosity fluids. III. Fully-developed flows. Rheol. Acta 25, 372–379.
White, F.M., 1999. Fluid Mechanics. McGraw-Hill, Singapore.
Whitehead, J.A., Helfrich, K.R., 1991. Instability of flows with temperature-dependent viscosity: a model of magma dynamics. J. Geophys. Res. 96 (B3), 4145–4155.
Wylie, J.J., Lister, J.R., 1995. The effects of temperature-dependent viscosity on a flow in a cooled channel with application to basaltic fissure eruption. J. Fluid Mech. 305, 239–261.